ELSEVIER

Journal of Chromatography A, 869 (2000) 339–352

JOURNAL OF CHROMATOGRAPHY A

www.elsevier.com/locate/chroma

Influence of flow patterns on chromatographic efficiency in centrifugal partition chromatography

L. Marchal[a,d], A. Foucault[a,*], G. Patissier[b], J.M. Rosant[c], J. Legrand[d]

[a]*Laboratoire de Biochimie et Molécules Marine, IFREMER, Nantes, France*

[b]*Laboratoire de Mécanique, IUT de Nantes, Nantes, France*

[c]*Laboratoire de Mécanique des Fluides, URM CNRS 6598, Ecole Centrale de Nantes, Nantes, France*

[d]*Laboratoire de Génie des Procédés, UPRES EA 1152, Université de Nantes, Saint-Nazaire, France*

Abstract

Visualization of flow patterns in centrifugal partition chromatography (CPC) was performed with an asynchronous camera and a stroboscope triggered by the CPC rotor, allowing a channel to be selected and observed regardless of rotational speed. Three main types of flow states were noted as a function of rotational speed and flow-rate: jets stuck along channel walls, broken jets and atomization. Our observations emphasize the importance of Coriolis force on flow shape. Chromatographic efficiency was related to the dispersion of the mobile phase in the stationary phase.

Keywords: Centrifugal partition chromatography; Efficiency; Flow patterns; Coriolis force

1. Introduction

Modern counter-current chromatography (CCC) originates from the pioneering studies of Ito et al. [1] who first constructed an apparatus in Japan designed to differentiate particles in suspension or solutes in solution in a solvent system subjected to a centrifugal acceleration field. This first machine led to two main applications: one, pursued by Ito in the USA, based on a wide variety of 'CCC apparati' using a variable-gravity field produced by a two-axis gyration mechanism and a rotary seal-free arrangement for the column; and the other, pursued by Nunogaki in Japan, based on 'centrifugal partition chromatography (CPC) apparati' and using a constant-gravity field produced by a single-axis rotation mechanism and two rotary-seal joints for inlet and outlet of the mobile phase. Several studies have been published [2–6] treating many examples of separations in various fields. Basically, CCC and CPC refer to support-free liquid–liquid chromatography with two immiscible liquids prepared by mixing two or more solvents or solutions. The instrument keeps one liquid stationary while the other is pumped through it, and the chromatographic process occurs between the two liquid phases. Despite improvements during the last twenty years, CCC and CPC instruments are still generally regarded as lacking efficiency, since more than one thousand theoretical plates are seldom encountered. It has often been claimed that this lack of efficiency is amply compensated by the high selectivity found in CCC and CPC (the two liquid phases can be finely tuned) and the high stationary-to-mobile phase ratio, which both have a positive effect on resolution [7,8]. However, as the efficiency of high-performance liquid chromatography has been

*Corresponding author.

0021-9673/00/$ – see front matter
PII: S0021-9673(99)01184-X

dramatically improved by a better knowledge of porous media (coarse or spherical beads, mono- or polydisperse beads, porous and non-porous material, pellicular and bulk material, etc.), ways need to be found to enhance the mass transfer between the two liquid phases in CCC and CPC in order to improve efficiency. In other words, resolution, R, can be seen as the sum of a physical contribution, i.e. efficiency, N, and stationary-to-mobile phase ratio, V_S/V_M, and of a chemical contribution, i.e. selectivity, α, and the average distribution ratio, D, of compounds of interest:

$$R = \left[N, \frac{V_S}{V_M} \right] \otimes [\alpha, D] \quad (1)$$

The first bracket is the task of the column manufacturer, the second that of the chromatographer.

The purpose of this study was to improve understanding of the influence of flow patterns on the chromatographic efficiency of CPC instruments (also called HDES instruments [2] or centrifugal droplet CCC [3]). Armstrong et al. [9] developed a mass transfer model to describe the efficiency of a CPC column as a function of the flow-rate of the mobile phase. They assumed that the bulk of the mass transfer occurs while the mobile phase is present as an emulsified band between the two phases. No visual evidence of the presence of such an emulsified band was presented. Foucault et al. [10] introduced the 'Stokes Model' which describes the flow of the mobile phase in a channel as droplets with an average radius corresponding to the Stokes Law. The average radius is calculated from the average linear velocity of the mobile phase in a channel, which in turn is calculated from stationary phase hold-up experiments [11]. The 'Stokes Model' is used to explain the stationary phase hold-up of various two-phase systems with different properties and the influence of rotational speed on efficiency. It was then suggested that a direct visualization of the mobile phase flow through the stationary phase would be very useful. Van Buel et al. [12] first presented photographs of the typical flow states of a CPC column for the hexane–water two-phase system at various flow-rates and rotational speeds. This work opened the way to a major contribution of Van Buel and co-workers for a better understanding of CPC [13–17]. Four main types of flow states were observed as a function of rotational speed and flow-rate: large droplets, a jet stuck along the channel walls, a broken jet, and atomization. The authors introduced the 'plug flow with axial dispersion' model, which allows the effluent concentration profile to be described as a function of indebted physical and chemical parameters. It was shown theoretically and experimentally that the inverse overall mass transfer coefficient, k_0, is a linear function of the distribution ratio, D, according to:

$$\frac{1}{k_0} = \frac{D}{k_M} + \frac{1}{k_S} \quad (2)$$

where k_M and k_S are the local mass transfer coefficients in the mobile and stationary phases. Furthermore, it was shown that the overall volumetric mass transfer coefficient, k_0a (a being the specific interfacial area between the stationary and mobile phases) depends on channel geometry.

Our work began at this point. In order to develop new CPC apparati, in collaboration with the French company SEAB, we set up a visualization system, to film flow patterns in a single channel of a transparent CPC prototype at any rotational speed. Our observations confirm those of Van Buel et al. [17], but also supplement them. Van Buel's observations were made in CPC channels parallel to the rotation axis $\vec{\Omega}$, so that flow patterns are described as seen in a plane parallel to $\vec{\Omega}$ (Fig. 1). Our observations were made in a plane perpendicular to $\vec{\Omega}$, so that in addition to the flow patterns described by Van Buel we observed deviations of jets or droplets from the radial direction, i.e. caused by forces perpendicular to $\vec{\Omega}$ and $\vec{V}_R$, the relative velocity of the mobile phase in the channel, such as Coriolis force [18]. In addition to these observations, the chromatographic efficiency of the CPC prototype was estimated from the peak shape for a given solute with a distribution ratio around 1 in the studied biphasic system. Another value than 1 could have been chosen, but the important point was to determine a value since the overall mass transfer coefficient (and thus the efficiency) is dependent on the distribution ratio, according to Van Buel's equation (Eq. 2). Further comparisons between different channels or different CPC instruments are possible only through this condition. A value of 1 is convenient for two reasons:

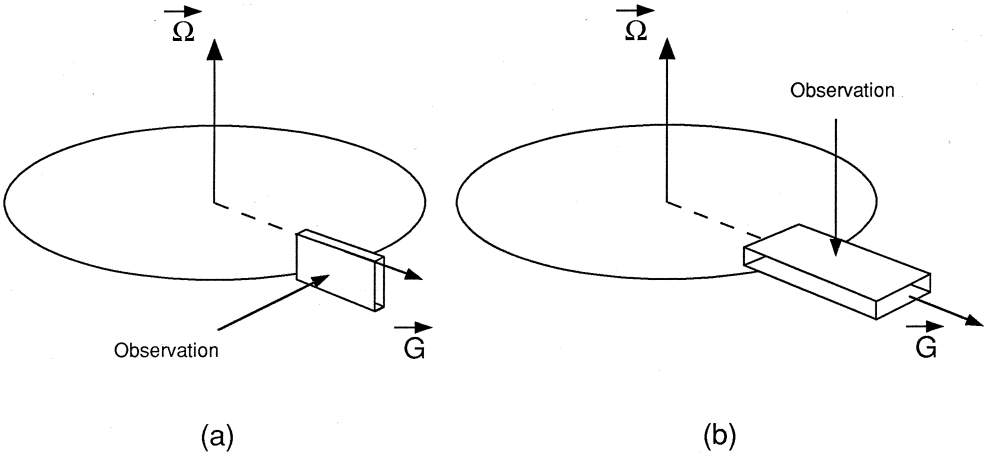

Fig. 1. Observation of flow patterns in CPC. (a) Observation in a plane parallel to the rotation axis (Van Buel et al. [17]); (b) observation in a plane perpendicular to the rotation axis (present study).

1. The retention volume for $D = 1$ corresponds to one column volume, regardless of the ratio of the mobile to the stationary phase [3].
2. It is widely accepted that it is good practice to choose a biphasic system in which a compound of interest has a distribution ratio around 1 to achieve its fast and efficient purification; it is then natural to estimate the efficiency of a CPC instrument around this value.

We report here some results obtained on one channel shape for several biphasic systems characteristic of the ones encountered in CPC, which emphasize the primordial importance of flow patterns on chromatographic efficiency.

2. Experimental

An overview of our experimental setup is shown in Fig. 2.

2.1. The visual CPC

The visual CPC consists of a body (steel) supporting an electrically driven asynchronous motor (Leroy Somer, Angoulême, France) and a vertical shaft bearing the CPC rotor with the upper side transparent. CPC channels were engraved in a 5-mm thick steel ring clamped between a steel plate and a glass ring of optical quality (Ediver, Rebais, France). A 0.05-mm-thick Teflon sheet (Angst+Pfister, Roissy-Charles de Gaulle, France) was tightened on each side of the engraved ring to ensure a leakage-free rotor. The engraved ring (175 mm I.D.×240 mm O.D.), had 66 parallelepipedic CPC channels of 10×4×5 mm connected by ducts 0.6 mm in width. The rotor was connected to the chromatographic system through 1/16 in. peek tubing (Upchurch Scientific, Oak Harbor, WA, USA) and two rotary seals (Tecmeca, Epernay, France) (1 in.=2.54 cm). The rotational speed could be varied from 0 to 3000 rpm.

2.2. Video-instrumentation

A slightly modified Videostrobe system was used (Sysmat Industrie, St Thibault des Vignes, France), consisting of a TMC-9700 progressive scan CCD digital color camera (Pulnix, Sunnyvale, CA, USA.) with an asynchronous shutter, two Phylec stroboscopic units (Sysmat) and a VLS7T optical speed sensor (Compact, Bolton, UK) which triggered both the stroboscopes and the camera. The camera was equipped with a 18–108 mm F 2.5 TV Zoom lens and connected to a CDM-810 multi-system converter (World Advanced Technologies, Toulouse, France), allowing NTSC/PAL/SECAM transcoding and 60/50 Hz field conversion. Images were recorded on an HR-DD946 MS video-recorder (JVC, Japan) monitored with a CPM1404 monitor (Hitachi, Japan), and/or on a computer equipped with a pentium 233

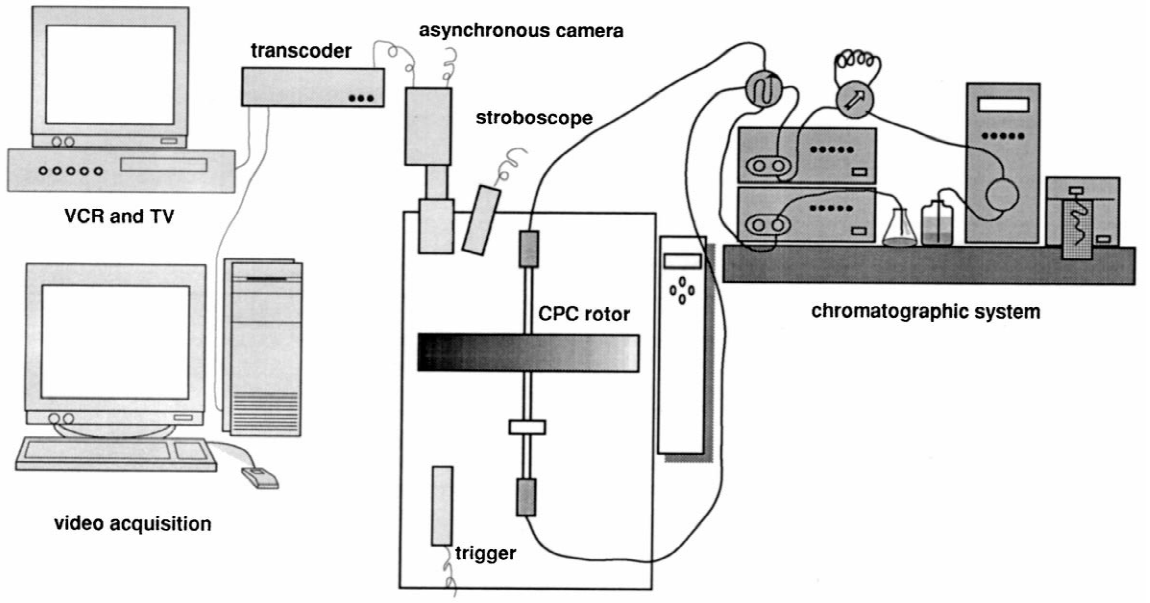

Fig. 2. Overview of the experimental setup, with the visualization system on the left, the 'visual CPC' in the center, and the chromatographic system on the right.

MHz processor and a Matrox Millenium II AGP power desk card (Matrox, Montreal, Canada) driven by MiroVideo DC30 Plus software (Pinnacle Systems, Mountain View, CA, USA). Films were stored using Adobe Premiere v. 4 (Adobe Systems, San Jose, CA, USA).

2.3. Chromatographic equipment

A P4000 quaternary gradient pump equipped with inert assemblies was used (ThermoQuest, San Jose, CA, USA), which delivered constant flow-rates from 0.1 to 30 ml/min. A 6-port injection valve and a 4-port switching valve, both in peek material (Upchurch), were used for injection and selection of either ascending (upper phase mobile) or descending (lower phase mobile) mode. Two Spectra 100 UV detectors equipped with 0–3 mm, 0–4.6 μl, variable pathlength preparative scale LC flowcells were used for chromatographic data acquisition (ThermoQuest). The first UV detector was positioned just after the injection valve and used to record the input profile of the injected sample. The second detector was conventionally positioned after the CPC column and used to record the output profile of the injected sample. The two profiles were acquired on a SA32 32-channel data acquisition system (AOIP, Evry, France), then exported onto a computer for further calculations.

2.4. Chemicals

Heptane, methanol, *n*-butanol and chloroform ('puro' grade) were from Carlo Erba (Rodano, Italy); and 2-propanol and dipotassium phosphate from Prolabo (Paris, France). Polyethylene glycol (PEG) 3350 and the various analytes used to generate chromatographic peaks were from Sigma (St. Louis, MO, USA). Water was deionized using a Milli-Ro4 water purification system (Millipore, Bedford, MA, USA).

2.5. Estimation of chromatographic efficiency

As initially reported by Scott and Kucera [19], complete injection of a sample loop results in a broadening of the injection profile, which affects the efficiency estimated through the chromatographic peak. In order to characterize the efficiency of our CPC column precisely, we inserted a UV detector

between the outlet of the injector and the inlet of the CPC column. A second detector was used to record the peak profile coming out of the column. The two signals were characterized by t_{inj}, δ_{inj}, t_R, δ_R, where t is the time for the peak-maximum and δ the peak-width at half-height for the injection signal and the eluted peak. Efficiency was then calculated by subtracting the dispersion due to the injection from that due to both the injection and the CPC column:

$$N = 5.54 \cdot \left(\frac{t_R - t_{inj}}{\delta_R - \delta_{inj}} \right)^2 \quad (3)$$

Eq. (3) is valid for Gaussian peaks and otherwise approximative; complete calculation (residence time distribution, RTD, and estimation of Péclet and Stanton number) will be reported elsewhere. A typical experiment is shown in Fig. 3. The scale for the abscissa is the dimensionless time defined by dividing the real time, t, by τ, defined as the detector 1 to detector 2 volume, V_c, divided by the flow-rate, F, and which equals the residence time for a compound with $D = 1$ ($\tau = 1158/F$, with F in ml/min and τ in seconds, for our experimental setup).

2.6. Characteristics of the biphasic systems studied

Five biphasic systems were selected for our experiments, which have their physical properties (interfacial tension, σ, density difference, $\Delta\rho$, viscosities of the two phases, η_{upper} and η_{lower}) close to those of most biphasic systems used for purification purposes; these properties are shown in Table 1. Systems were classified according to the Ohnesorge number of the upper phase ($Z = \eta_{upper}/\sqrt{\rho_{upper}\sigma L}$), where L is a characteristic length, i.e. the duct width

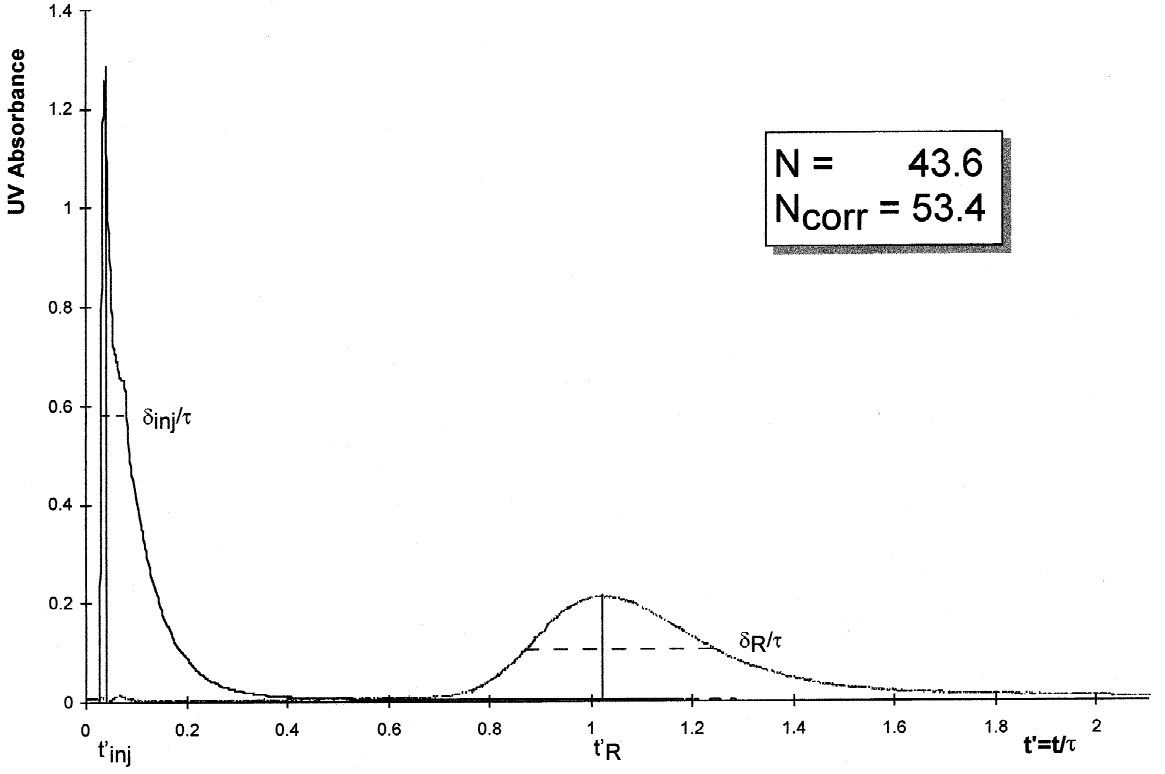

Fig. 3. Standard procedure to estimate the efficiency of the CPC column: the injection peak is recorded by a first detector positioned just after the sample loop; τ is the residence time of a solute with a distribution ratio of 1 ($\tau = V_C/F$, where V_C = column volume ≈ detector to detector volume, F = flow-rate) N_{corr} corresponds to Eq. 3; N is calculated using the elution peak alone (*n*-butanol–acetic acid–water system, with Leu–Tyr as a peakmaker, ω = 1500 rpm, F = 15 ml/min, descending mode).

Table 1
Physical properties of the biphasic systems; the Ohnesorge number characterizes atomization properties. The peak-maker is used to generate a chromatographic peak and estimate the efficiency[a]

Systems	ρ Density g/cm^3 UP	ρ Density g/cm^3 LP	$\Delta\rho$ Difference g/cm^3	σ Interfacial tension mN/m	η Viscosity cP UP	η Viscosity cP LP	Z Ohnesorge number AM	Peak maker
Hep/W	0.679	0.997	0.318	44	0.41	1.33	0.003	–
Hep/MeOH	0.684	0.756	0.072	1.16	0.47	0.65	0.022	Phenyl salicylate
HCPMW	0.939	1.037	0.098	–	1.46	0.60	–	*p*-Hydroxybenzoic acid methyl ester
BAW	0.891	0.992	0.101	1.21	2.48	1.51	0.098	Leu–Tyr
CPMW	0.968	1.181	0.213	0.42	1.78	0.97	0.114	*p*-Hydroxybenzoic acid methyl ester
ATPS	1.086	1.13	0.044	0.37	19.96	1.23	1.285	Lysosyme

[a] Abbreviations: UP: upper phase; LP: lower phase; AM: ascending mode; Hep/W: heptane–water; Hep–MeOH: heptane–methanol; HCPMW: heptane–chloroform–*n*-propanol–methanol–water (20–23.2–5.2–31–20.6); BAW: *n*-butanol–acetic acid–water (40–10–50,); CPMW: chloroform–*n*-propanol–methanol–water (29–6.5–38.7–25.8); ATPS: aqueous two phase system made of polyethylene glycol 3550–dipotassium phosphate–water (17.4–10.6–72, w/w).

in our works. Z [viscous force/(inertia force·interfacial force)$^{1/2}$] characterizes the atomization properties, i.e. easiness to disperse one phase into another. Selected systems had their interfacial tension in the 0.4 to 3 mN/m range and their Z values in the 0.02–0.11 range. The aqueous two-phase system (ATPS) appeared to be apart from other systems ($Z = 1.3$); we selected it for further study of this particular field of CPC purification of proteins and other biopolymers. The biphasic heptane–water system shown for comparison in Table 1 appears to be very far from the range of other biphasic systems; its very large interfacial tension and consequently its very low Z number make it unsuitable for hydrodynamic studies since flow patterns obtained with this system are totally different from those encountered in biphasic systems useful for CPC[1].

3. Results and discussion

Our studies confirm Van Buel's observations and also emphasize the importance of Coriolis force on flow shape. Except when stuck against walls, jets deviate considerably from the radial direction before breaking. Chromatographic efficiency is largely due to the good mixing of the two phases in each channel. Visualization of flow patterns allowed us to verify this and elucidate previous assumptions based on studies of various relationships between efficiency and several parameters [9,10].

3.1. Heptane–methanol system, descending mode

This system has been studied for flow-rates in the 3–24 ml/min range and rotational speeds in the 400–1500 rpm range (results are summarized in Figs. 4–7). Four main flow patterns were observed: (1) a jet stuck along one or two walls; (2) a curvilinear jet; (3) sinuous and varicose breakup; (4) atomization.

The change in configuration from 1 to 4 results in better mixing and corresponds to an increase in efficiency (Fig. 5). This corresponds to an increase of ω and/or F (Fig. 6). Typically, for a flow-rate of 9 ml/min, two jets stuck on each side of the channel and with a wavy surface were observed at a rotational speed of 300 to 500 rpm. At around 500 rpm one of the two jets came unstuck due to the Coriolis force and crossed the channel. From 600 to 1100 rpm, a curvilinear jet occurred, which broke upon reaching the wall and then streamed down. Beyond 1100 rpm, a sinuous or varicose breakup configuration appeared, producing droplets too small to be

[1] The heptane–water system gives stuck or unbroken jets whatever F and ω are, in the studied channels [20].

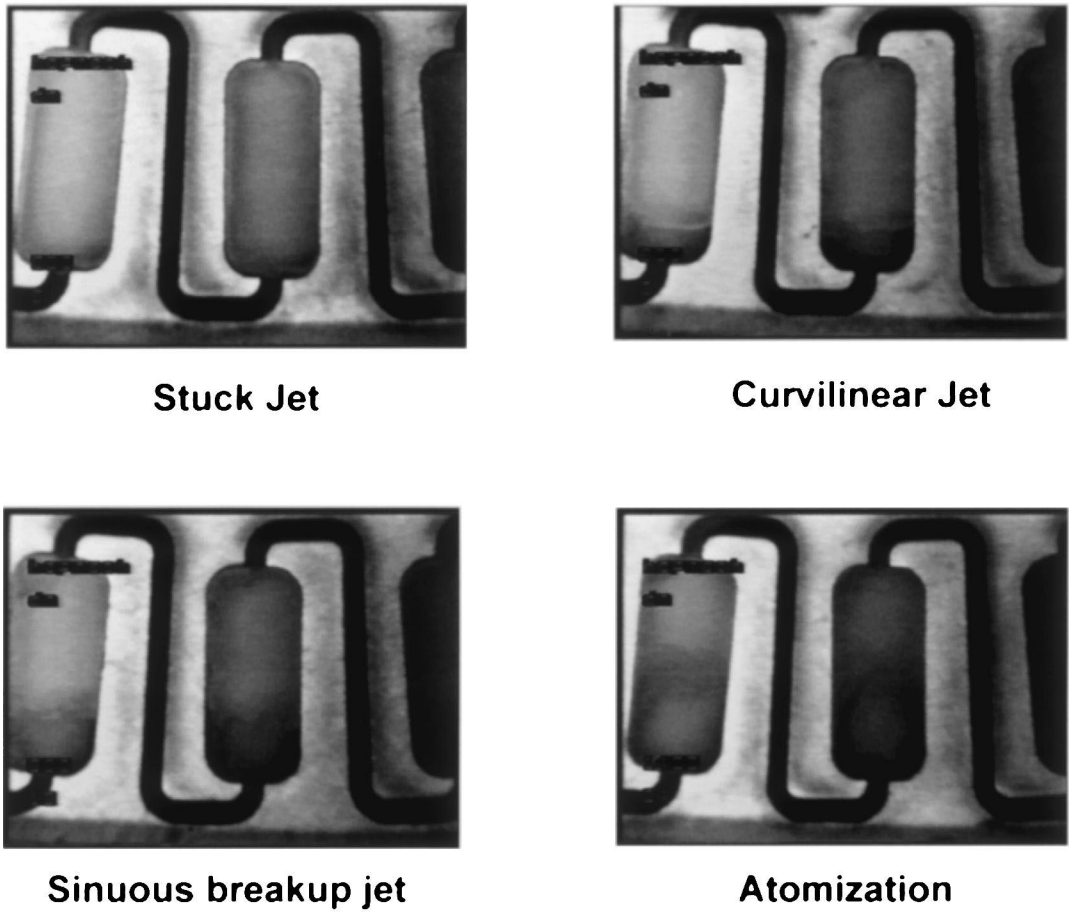

Fig. 4. Flow patterns observed in CPC. Heptane–methanol system, descending mode. The mobile phase looks darker than the stationary phase (top left: 1). Stuck jets along the walls ($F = 6$ ml/min, $\omega = 500$ rpm) (top right: 2). Curvilinear jets ($F = 9$ ml/min, $\omega = 600$ rpm): jet deviated on the right according to its relative velocity and to Coriolis force for a trigonometric rotation (bottom left: 2). Sinuous or varicose breakup ($F = 18$ ml/min, $\omega = 600$ rpm): indistinguishable droplets are generated by the broken jet, giving a darker image in the channel (bottom right: 4). Atomization ($F = 24$ ml/min, $\omega = 1400$ rpm). Fine droplets are generated at the inlet of the channel (top), giving a scintillating and dark pattern to the channel. They coalesce at the bottom, giving a darker pool of mobile phase with a chaotic surface.

individually characterized but giving a scintillating image in the channel (or a gray color between the light gray of the stationary phase and the dark gray of the mobile phase in Fig. 4). At a higher rotational speed, the broken jet disappeared, and full atomization occurred. The rotational speed at which a transition occurred was dependent on the flow-rate, as shown in Fig. 7. This flow-chart is characteristic of a given biphasic system for a given mode and for a given channel shape.

Remarks. (1) Peaks recorded at lower rotational speeds are not Gaussian and correspond to the stuck-jet configuration; peaks suddenly become Gaussian when jets come unstuck from the walls.

(2) The best efficiencies correspond to 110–150 theoretical plates given by 66 channels, i.e. 0.6 to 0.44 channel per plate (a concept introduced by Armstrong [9] and comparable to the reduced plate height). This means that the channel profile used in this study, though non-optimized, appears to be much more efficient than those commercially available (channel per plate always greater than 1) ([9,10]).

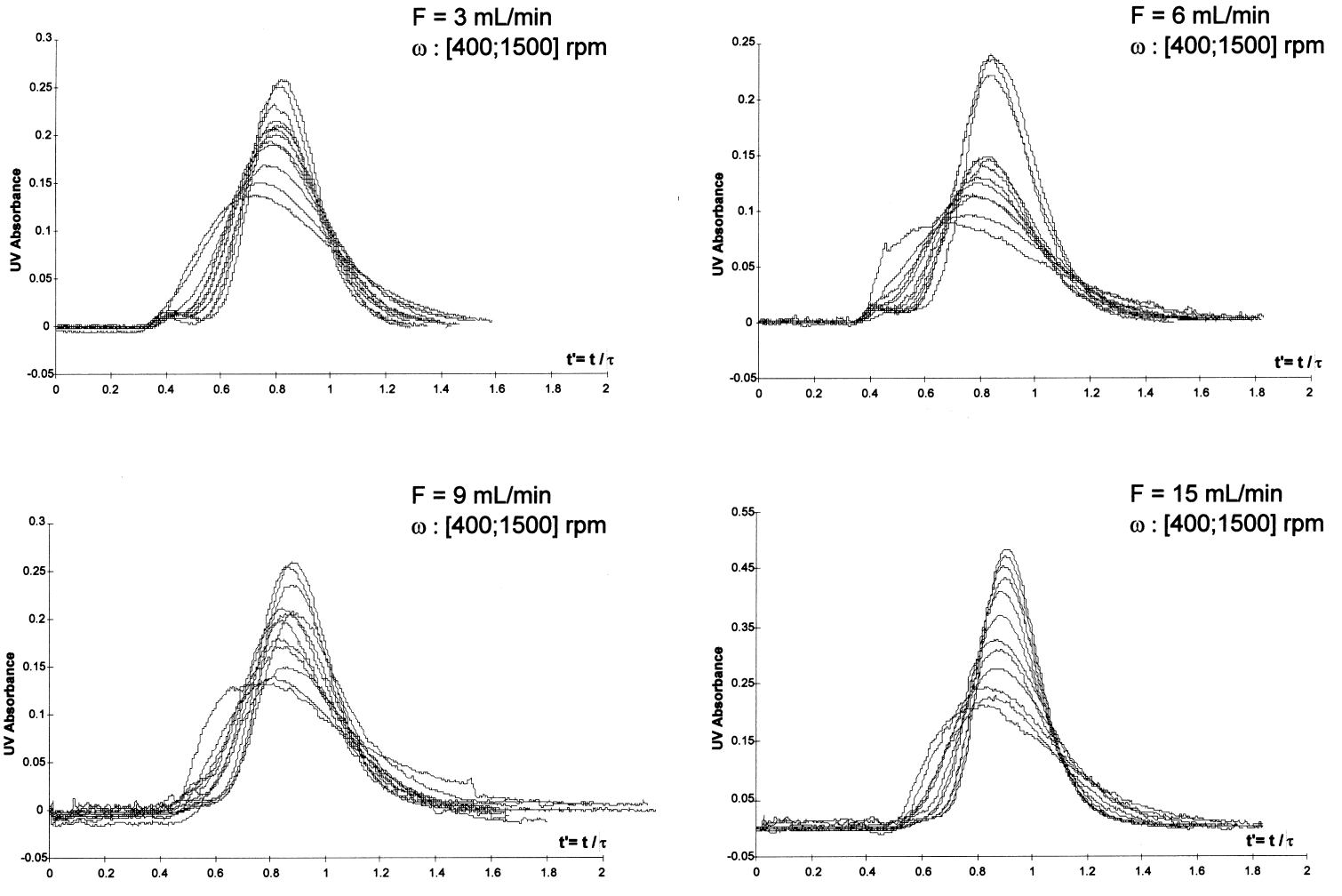

Fig. 5. Changes in peak shapes with F and ω. Heptane–methanol, descending mode. Peak maker: phenyl salicylate. Non-Gaussian peaks correspond to the stuck-jet configuration. Efficiency increases from flow configuration 1 to flow configuration 4 on Fig. 4.

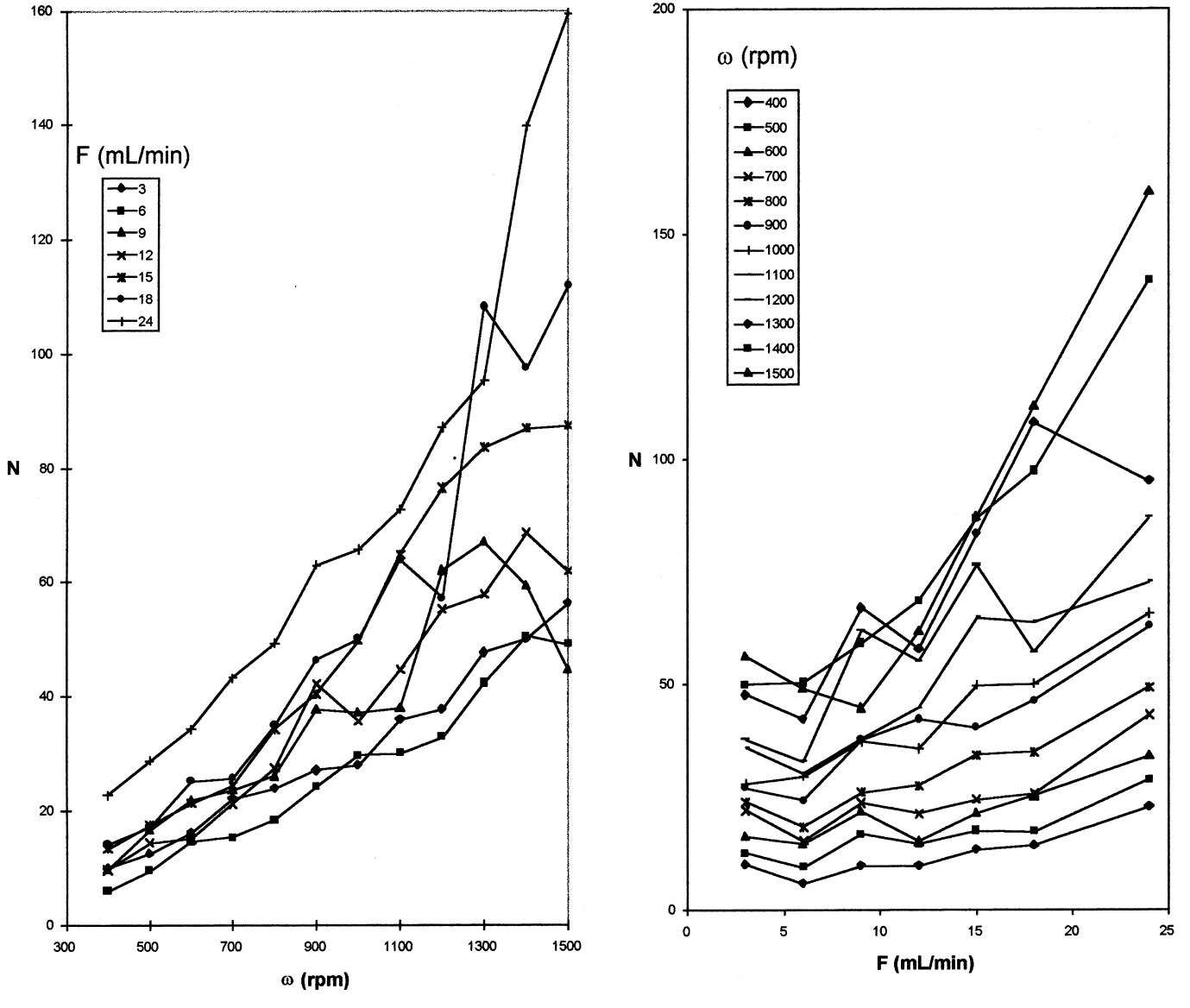

Fig. 6. Efficiency as a function of F and ω. Heptane–methanol system, descending mode. Peak maker: phenyl salicylate. General tendency is an increase in efficiency with F and ω.

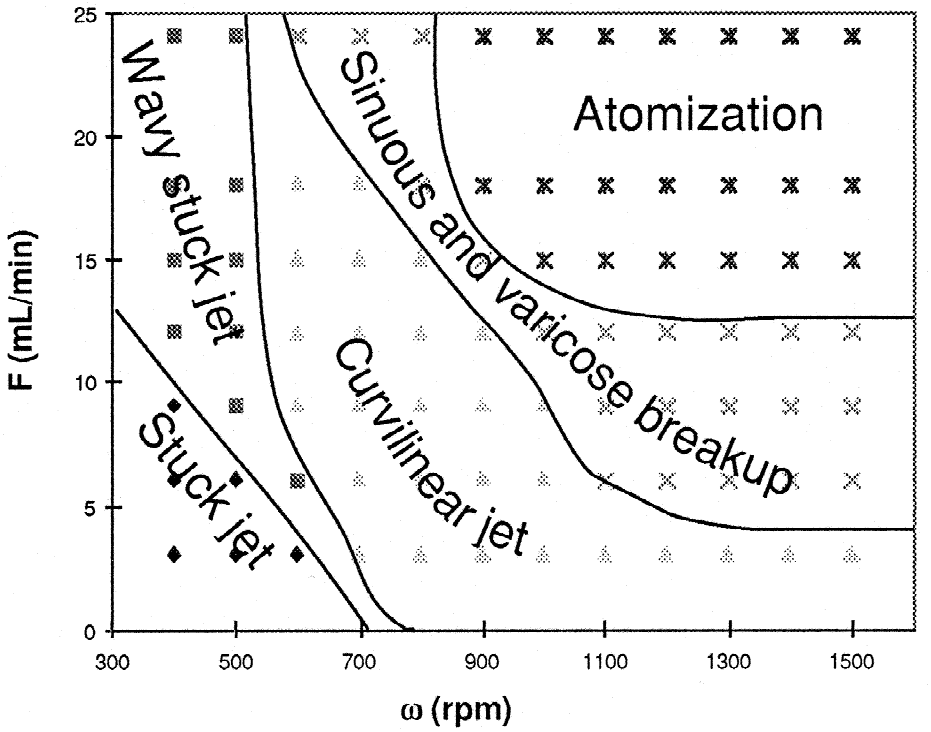

Fig. 7. Flow-chart for the heptane–methanol system in the descending mode. A flow-chart is characteristic of a given biphasic system in a given mode and for a given channel shape.

3.2. Chloroform–n-propanol–methanol–water system

This is the less stable system studied by Foucault et al. [10]. When looking at flow patterns for this system, it appears that atomization occurs very early. For $\omega = 1200$ rpm and $F = 3$ ml/min in both modes, complete atomization is seen in the channels, while for the same conditions with the heptane–methanol system, a non-broken curvilinear jet configuration was observed. Attempts to increase F resulted in large bleeding and rapid removal of the entire stationary phase from the channels. The easiness to atomize one phase was characterized by the Ohnesorge number (Table 1), which can be used to make certain predictions. Bleeding occurred because coalescence was not fast enough to produce a homogeneous mobile phase layer at the outlet of the channel, but this could be overcome by modifying the geometry of the CPC channels.

3.3. Heptane–chloroform–n-propanol–methanol–water system

Heptane was added to the previous system to obtain (1) a more stable biphasic system and (2) a distribution ratio of 1 for the *p*-hydroxybenzoic acid methyl ester chosen as the peakmaker (i.e. the solute which generates a chromatographic peak). The resulting system is representative of several used in CPC, such as alkane–alcohol–water or chlorinated solvent–alcohol–water, or any system with medium polarity widely used for purification purposes. The following example highlights the difference in efficiency found between ascending and descending modes. Fig. 8 shows peaks obtained for $\omega = 1200$ rpm and $F = 15$ ml/min, and flow patterns corresponding to these experiments. Although the flow patterns are quite similar, corresponding to the sinuous breakup configuration, efficiency ranges from 10 (6.6 channels per plate) to 42 (1.6 channels

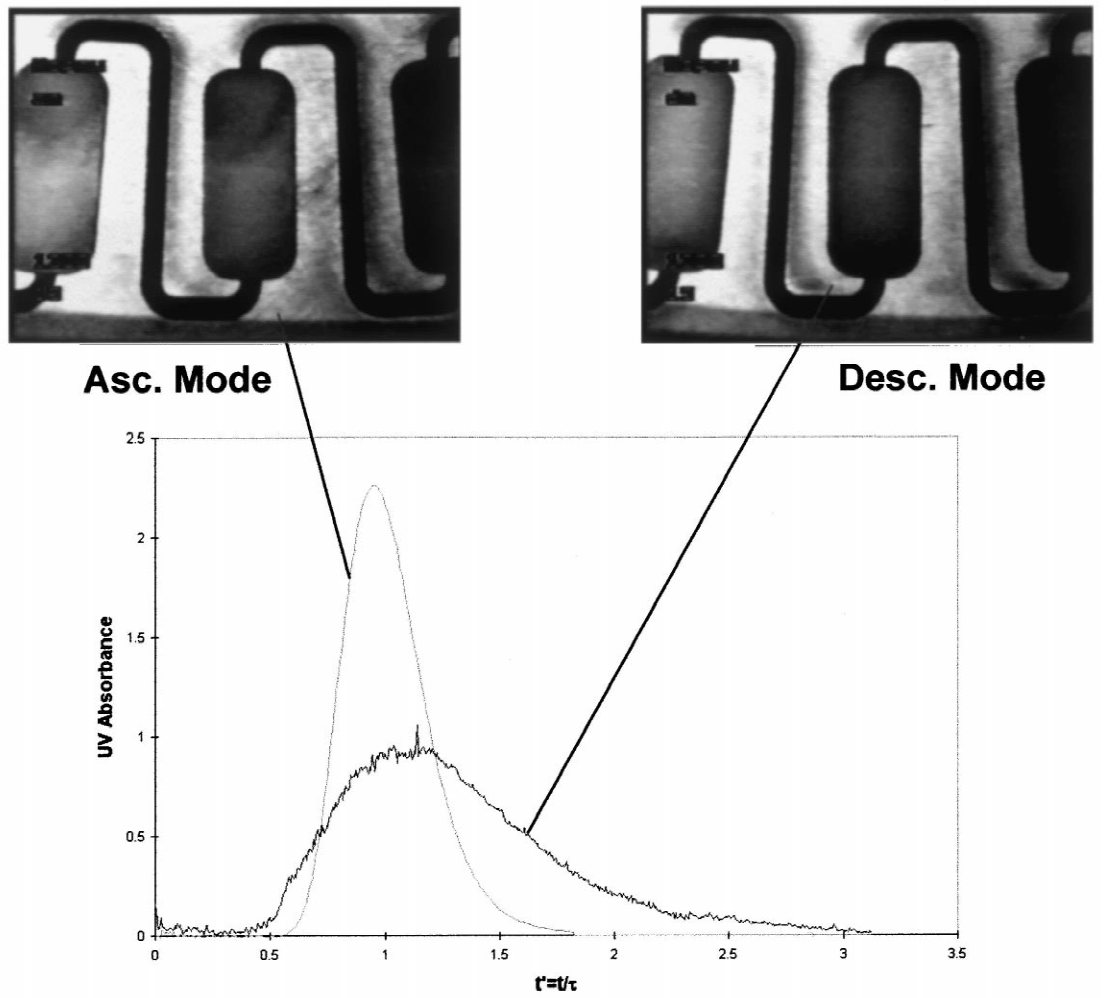

Fig. 8. Comparison between efficiencies observed in the ascending and descending modes for similar flow patterns: heptane–chloroform–*n*-propanol–methanol–water system, with *p*-hydroxybenzoic acid methyl ester as peak maker; $F = 15$ ml/min; $\omega = 1200$ rpm.

per plate). This large difference between modes, which occurred for other systems experimented in our study, does not seem to have been reported previously since most experiments have been performed in only one mode [9,10,16]. It is not clear why the ascending mode is more efficient than the descending mode. Further studies are needed since the flow patterns do not seem to be involved in this particular case. An explanation could be found looking at differences in diffusive properties in the two phases, partly controlled by viscous forces.

3.4. n-Butanol–acetic acid–water system

This system has been extensively used by Knight [21] and many other scientists to purify peptides and analogs. In this system the dipeptide Leu–Tyr has a distribution ratio of exactly 1, which makes it very useful for estimations and comparisons. In this experiment, we found that low rotational speeds and low flow-rates in CPC resulted not only in a serious loss of efficiency but also generated short-circuit zones, i.e. zones in which the solute never goes. In

other words, there are conditions in which the mobile phase goes through the CPC column by following 'preferential paths.' This is shown in Fig. 9 in which peaks corresponding to Leu–Tyr have been recorded for $F=9$ ml/min and $\omega=400$–1500 rpm in both modes. At lower rotational speed, the main part of the injected solute comes out earlier than expected ($t_R/\tau=0.6$ instead of 1), followed by a flat and long tail. This corresponds to a stuck-jet configuration. By increasing ω, the peak becomes Gaussian and centered at $t_R/\tau=1$. This corresponds to a better dispersion of the mobile phase, and probably to better recirculating zones for the stationary phase. As in the previous experiment, the efficiency reached in the ascending mode is better than that reached in the descending mode. This shows the fundamental role of rotational speed in CPC, which contributes not only to ensuring the retention of the stationary phase but also plays a major role in the quality of mass transfer during the chromatographic process.

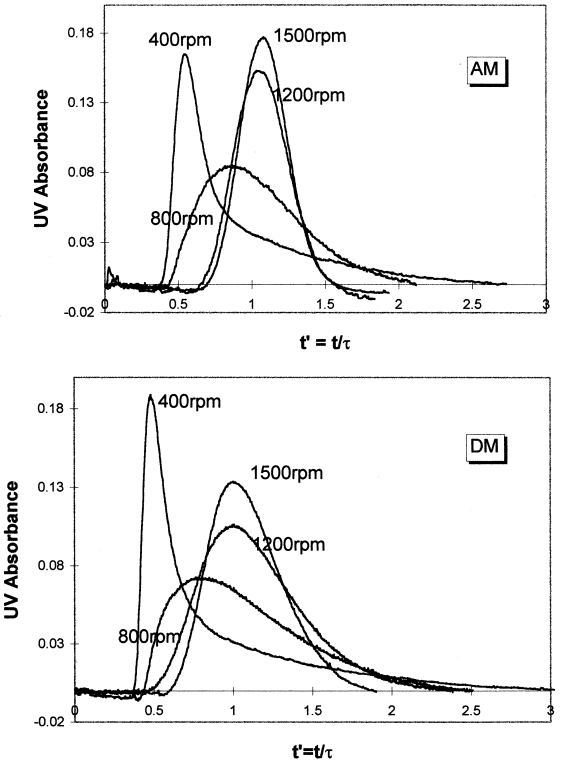

Fig. 9. Evidence of short-circuit zones in CPC: *n*-butanol–acetic acid–water system, with Leu–Tyr as a peak maker; $F=9$ ml/min, ω and mode as indicated. Leu–Tyr has a distribution ratio of 1, but at lower rotational speeds a peak appears earlier than expected, followed by a long and flat tail. This corresponds to short-circuit zones (preferential paths), i.e. stationary phase zones where the solute never goes.

3.5. Aqueous two-phase systems

These systems are very useful for purification of proteins and other biomolecules, but are rarely used in CPC where they generally allow broad peaks to be obtained [22]. They are characterized by a very small density difference and interfacial tension, and a large viscosity of the polymer phases. We experimented PEG 3350-phosphate buffer, pH 11, in which the viscosity of the upper phase is around 20 cP, while that of the lower one is around 1.2 cP. In this system, lysozyme has a distribution ratio of around 1. However, when operating in the descending mode, lysozyme is eluted as a small peak coming out at the void volume (i.e. the volume occupied by the mobile phase in the CPC column), followed by a flat and long tail sometimes merely discernable from the baseline. Lysozyme regularly comes out at $t_R/\tau\approx1$ in the ascending mode (Fig. 10). The flow conditions ($F=9$ ml/min, $\omega=1200$ rpm) correspond to an atomization in the descending mode and to a curvilinear jet in the ascending mode. We suspect that for the descending mode the viscous stationary phase is short-circuited by the mobile phase, while the expected mass transfer between the two phases occurs when the less viscous phase is the stationary phase. Attempts at improving mass transfer in the descending mode by increasing F and/or ω resulted in a complete loss of the stationary phase due to a severe bleeding. It is noteworthy that the efficiency obtained in the ascending mode (53 theoretical plates, 1.24 channel per plate) was much higher than that previously observed for this kind of application [22].

4. Conclusion

Visualization of flow patterns in CPC confirmed the general assumption that a better mixing of the two phases in channels leads to better efficiency and confirmed the primary role of flow-rate and rotational speed as the key parameters acting on this mixing. The earlier the mobile phase jets are broken, the better the result, provided that coalescence is fast enough to prevent constant bleeding of the stationary

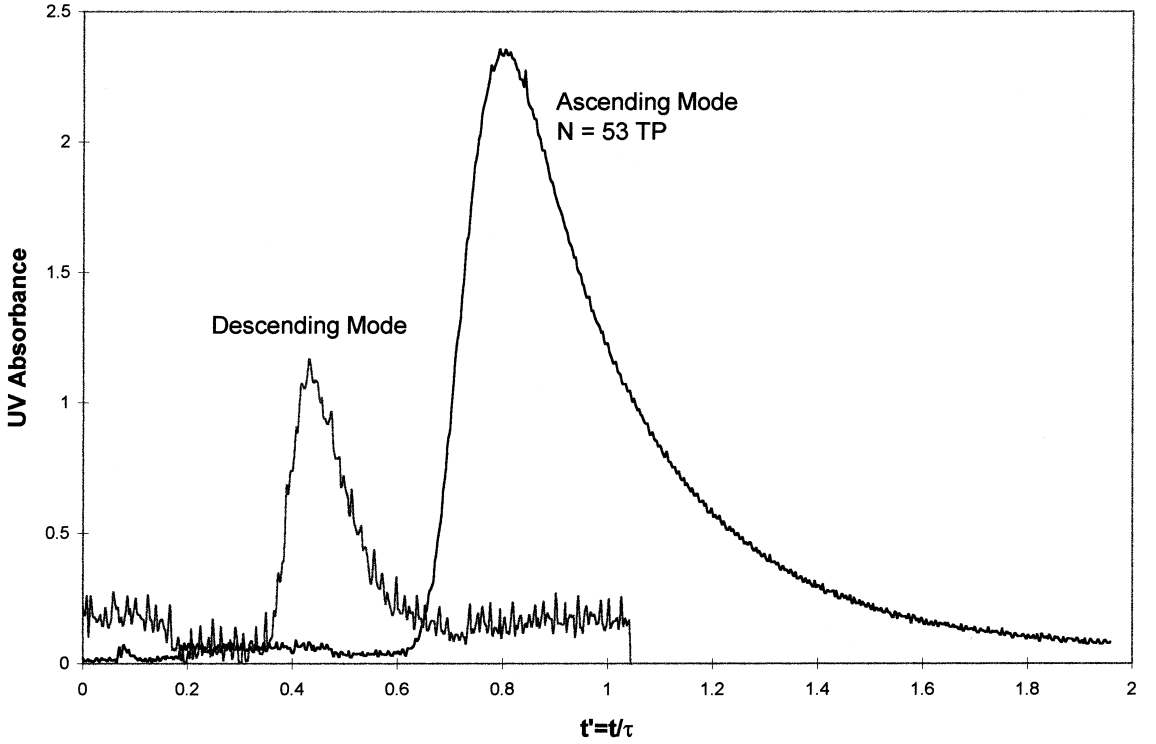

Fig. 10. Evidence of short-circuit zones in CPC. Aqueous two-phase system, with lysozyme as a peak maker; $F = 9$ ml/min, $\omega = 1200$ rpm. Lysozyme has a distribution ratio of around 1, but in the descending mode it appears as a small peak coming out at the void volume, followed by a flat and long tail merely discernible from the noisy baseline.

phase by mechanical drive. However, a question arises from our results relative to the difference observed between ascending and descending modes for a given system. Is this behavior pattern caused by the difference in viscosities of the two phases or by other parameters? This study has concerned only one channel shape, but it may be easily understood that channel shape has a great influence on flow patterns. Further experiments with various channel shapes designated for general or specific applications (such as use with aqueous two-phase systems) are now in progress, and our results will be reported later [23].

Acknowledgements

This study was supported by ANVAR (French Agency for the Development of Industrial Innovation), IFREMER (French National Research Institute for Exploitation of the Sea) and CNRS (French National Center for Scientific Research).

References

[1] Y. Ito, M. Weinstein, I. Aoki, R. Harada, E. Kimura, K. Nunogaki, Nature 212 (1966) 985.
[2] Y. Ito, B. Mandava (Eds.), Counter-current Chromatography — Theory and Practice, Chromatographic Science Series, Vol. 44, Marcel Dekker, New York, 1988.
[3] W.D. Conway, Counter-current Chromatography—apparatus, Theory and Applications, VCH, New York, 1990.
[4] A.P. Foucault (Ed.), Centrifugal Partition Chromatography, Chromatographic Science Series, Vol. 68, Marcel Dekker, New York, 1994.
[5] W.D. Conway, R.J. Pwetroski (Eds.), Modern Counter-current Chromatography, ACS Symposium Series, Vol. No. 593, American Chemical Society, Washington, DC, 1995.
[6] Y. Ito, W.D. Conway (Eds.), High-speed Counter-current Chromatography, Chemical Analysis, Vol. 132, Wiley, New York, 1996.
[7] R. Margraff, A.P. Foucault (Eds.), Centrifugal Partition Chromatography, Chromatographic Science Series, Vol. 68, Marcel Dekker, New York, 1994, p. 331, Chapter 12.
[8] A.P. Foucault, L. Chevolot, J. Chromatogr. A 808 (1998) 3.
[9] D.W. Armstrong, G.L. Bertrand, A. Berthod, Anal. Chem. 60 (1988) 2513.

[10] A.P. Foucault, E. Camacho-Frias, C.G. Bordier, F. Le Goffic, J. Liq. Chromatogr. 17 (1994) 1.
[11] A.P. Foucault, O. Bousquet, F. Le Goffic, J. Liq. Chromatogr. 15 (1992) 2691.
[12] M.J. Van Buel, L.A.M. Van den Wielen, K.Ch.A.M. Luyben, in: A.P. Foucault (Ed.), Centrifugal Partition Chromatography, Chromatographic Science Series, Vol. 68, Marcel Dekker, New York, 1994, p. 51, Chapter 3.
[13] M.J. Van Buel, L.A.M. Van den Wielen, K.Ch.A.M. Luyben, J. Chromagogr. A 773 (1997) 11.
[14] M.J. Van Buel, L.A.M. Van den Wielen, K.Ch.A.M. Luyben, J. Chromagogr. A 773 (1997) 13.
[15] M.J. Van Buel, L.A.M. Van den Wielen, K.Ch.A.M. Luyben, AIChE J. 43 (1997) 693.
[16] M.J. Van Buel, Thesis, Delft University of Technology, Delft, 1997.
[17] M.J. Van Buel, F.E.D. Van Haldema, L.A.M. Van den Wielen, K.C.A.M. Luyben, AIChE J. 44 (1998) 1356.
[18] A.P. Foucault, L. Marchal, J.M. Rosant, S. Farias Neto, J. Legrand, P. Durand, presented at the 1998 Pittsburgh Conference, New Orleans, 1998, Abstract 878.
[19] R.P.W. Scott, P. Kucera, J. Chromatogr. 119 (1976) 467.
[20] A. Morvan, L. Marchal, A.P. Foucault, unpublished results.
[21] M. Knight, in: Y. Ito, B. Mandavas (Eds.), Counter-current Chromatography—theory and Practice, Chromatographic Science Series, Vol. 44, Marcel Dekker, New York, 1988, p. 583, and references therein.
[22] A. Foucault, K. Nakanishi, J. Liq. Chromatogr. 13 (1990) 2421.
[23] A. Morvan, A. Foucault, G. Patissier, J.M. Rosant, J. Legrand, presented at the 2nd European Congress of Chemical Engineering, Montpellier, 5–7 Oct., 1999.